JACS
JOURNAL OF THE AMERICAN CHEMICAL SOCIETY
pubs.acs.org/JACS
Article

Tuning Electrocatalytic Oxygen Reduction Reaction with Dynamic Control of Electrochemical Interfaces

Hyein Lee and Hang Ren*

Cite This: https://doi.org/10.1021/jacs.3c13694
Read Online
ACCESS | Metrics & More | Article Recommendations | Supporting Information

ABSTRACT: Herein, we report the tuning of the activity and selectivity of the oxygen reduction reaction (ORR) through the dynamic regulation of the electrochemical interfaces to surpass the performance of conventional electrocatalysis. This is achieved by applying an oscillating potential between the ORR operating potential and anion adsorbing potential on a gold electrode. Oscillating potential enhances the selectivity for H_2O_2 by up to 1.35 times compared to the static potential, as confirmed by rotating ring-disk electrode and fluorescence assay measurements. We showed that the enhanced selectivity depends on dynamic adsorption and desorption of anions, and the enhancement occurs in the millisecond time scale or shorter. The transient selectivity to H_2O_2 can reach ~97% within the first 5 ms after potential switching. Our results suggest that the dynamic interface can create a transient but unique microenvironment for new reactivity that cannot be reproduced under static conditions, which offers a new dimension in controlling electrocatalysis.

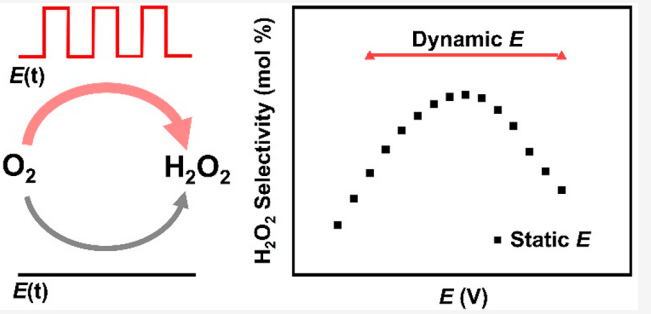

INTRODUCTION

Electrocatalysis is of great significance in energy conversion and storage, as well as chemical synthesis.[1−3] Enhancing the catalytic activity and product selectivity are two important objectives.[4] Extensive endeavors have focused on fine-tuning the binding energy at the active sites to optimize electrocatalytic reactions.[5] However, Nørskov and co-workers have shown that this approach is fundamentally limited by the scaling relationship: the binding energy of each intermediate cannot be independently optimized to achieve their individual optimum.[6,7] Overcoming the scaling relationship poses a fundamental challenge in the catalyst design.

One promising approach to control electrocatalysis beyond optimizing the binding energy at the static active site is to dynamically tune the property of the electrochemical interface.[8−10] One facile way is to dynamically alter the electrode potential. Indeed, oscillating potential, also often known as pulsed electrocatalysis, has been shown to increase the activity of electrochemical formic acid oxidation and change the selectivity of the CO_2 reduction reaction (CO_2RR).[11−14] Additionally, Qin and co-workers have demonstrated the enhanced production rate of H_2O_2 during oxygen reduction reaction (ORR) on graphite felt and porous carbon with potential oscillation.[15,16] The altered activity is often attributed to factors including the dynamic surface structure,[13] enhanced mass transport,[15] and the electrical double-layer effect.[16] However, the complicated surface structure, uncontrolled mass transport, and convolution of Faradaic and non-Faradaic currents in these dynamic conditions make it challenging to determine the intrinsic selectivity of the electrocatalytic reactions and to elucidate the key factors determining the interfacial reactivity. The lack of this mechanistic insight hinders the rational design of dynamic interfaces for electrocatalysis.

ORR can produce H_2O or H_2O_2 as the major products, which can serve as a testbed to understand activity and selectivity in electrocatalysis.[17] The bifurcation between H_2O_2 vs H_2O pathways is determined by the bond cleavage of the *OOH intermediate: breaking the *−OOH vs the *O−OH bond will lead to H_2O_2 vs H_2O, respectively.[16] In principle, secondary adsorbed species, e.g., anions, can either distabilize *OOH or help protonate the surface-bound O atom of *OOH, favoring *OOH desorption and H_2O_2 generation. However, at static ORR operating potentials, the coverage of these secondary species is either too high to block ORR, or too low to be effective. We hypothesize dynamically changing the potential can transiently create an interfacial environment that is not obtainable under static conditions, which can better tune the activity and selectivity in ORR.

Received: December 5, 2023
Revised: April 8, 2024
Accepted: April 8, 2024

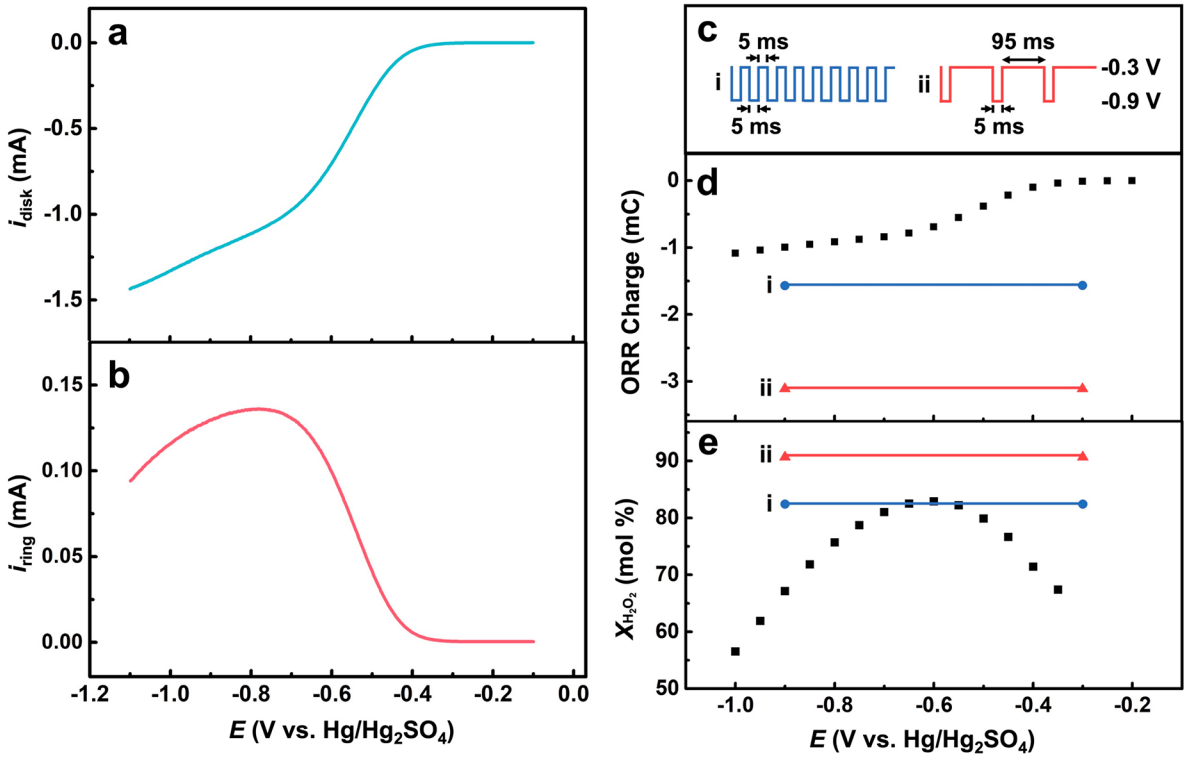

Figure 1. (a) Linear sweep voltammogram of the Au disk of RRDE (disk: Au, ring: Pt) in 100 mM phosphate buffer (pH 7.4) saturated with O_2. ν = 5 mV/s. (b) Corresponding Pt ring current at 0.2 V for H_2O_2 oxidation during the voltammetric scan on the disk. (c) Two dynamic potential waveforms used that oscillate between −0.3 and −0.9 V (vs Hg/Hg_2SO_4). (d) ORR charge under static potential (dots) and dynamic potential oscillation (horizontal lines). (e) Mole fraction of H_2O_2 ($X_{H_2O_2}$) in the ORR under static potentials (dotted lines) and dynamic potential oscillations (horizontal lines). The duration of the static potential is 0.75 s and the dynamic potential of (i) and (ii) are 1.5 and 15 s, respectively. Collection efficiency of the RRDE is 18.3%. Rotation rate: 1200 rpm.

In this paper, we test the hypothesis of using the dynamic electrochemical interface to tune the selectivity using ORR as the model reaction. The dynamic interface is created by alternating the electrode in two states via potential oscillation: at a more positive potential, ion adsorption on the electrode is promoted transiently, and at a more negative potential, the ORR is promoted. Rotating disk electrodes (RDE) and rotating ring disk electrodes (RRDE) allow precise control of mass transport, and RRDE allows the measurement of the selectivity of H_2O_2 during dynamic electrocatalysis, which is further confirmed by fluorescence assays. We experimentally revealed that the role of anion adsorption is important in determining the transiently enhanced selectivity. By carefully deconvoluting the non-Faradaic and Faradaic reactions with the aid of finite element simulation, we quantitatively show that the enhanced H_2O_2 selectivity occurs during the transient region. The selectivity at this short time scale (ms) is further experimentally quantified by the single potential pulse experiment.

RESULTS AND DISCUSSION

The electrocatalytic activity and selectivity in ORR were first studied under static conditions using RRDE. The potential on the Au disk was swept from −0.1 to 1.1 V (vs Hg/Hg_2SO_4) to induce ORR, while the Pt ring was held at 0.2 V (vs Hg/Hg_2SO_4) to oxidatively collect H_2O_2 at mass transport limited rate (Figure S1). The voltammogram in Figure 1a shows that when the potential on Au is more negative than −0.4 V, the current increases, corresponding to the ORR. The corresponding ring current increases with the ORR current on the disk, validating the generation of H_2O_2 from the ORR on Au (Figure 1b). As the potential reaches more negative than −0.8 V, the ORR current continues to increase while the H_2O_2 production decreases, suggesting a transition from a 2-electron to 4-electron pathway, consistent with the previous reports.[18,19] The ORR activity and selectivity were also studied via potentiostatic coulometry to facilitate a comparison with dynamic conditions (vide infra). The charge on the disk (Q_{disk}) reflects ORR activity, while the charge on the ring (Q_{ring}) can be used together with Q_{disk} to calculate the mole fraction of H_2O_2 in the product ($X_{H_2O_2}$) using

$$X_{H_2O_2} = \frac{Q_{ring}/2\eta}{Q_{ring}/2\eta + (Q_{disk} - Q_{ring}/\eta)/4} \quad (1)$$

In eq 1, η is the collection efficiency of the RRDE, which is 18.3% as calibrated by voltammetry using ferrocyanide (Figure S4). The ORR activity and H_2O_2 selectivity measured from the coulometry are consistent with the voltammograms in Figure 1a–b. As shown in Figure 1d–e, as the potential becomes more negative, the ORR activity increases, while H_2O_2 selectivity (as measured by $X_{H_2O_2}$) under static potential conditions first increases and then decreases, reaching a maximum of 83.1 ± 0.2% at −0.6 V.

To study the effect of the dynamic interface on the ORR, the potential on the disk is stepped between two values at a specific frequency, corresponding to a square wave, while the ring is held at 0.2 V to collect H_2O_2 similar to the static

https://doi.org/10.1021/jacs.3c13694
J. Am. Chem. Soc. XXXX, XXX, XXX−XXX

condition. The upper potentials were chosen to avoid both the oxidation of the Au electrode and the product of H_2O_2, which is guided by the voltammetric experiments as shown in Figures S2 and S3. When the potential oscillates between −0.3 and −0.9 V at 100 Hz with the duration for the upper and lower potential of 5 ms in one period(Figure 1c(i)), the total ORR charge (curve i in Figure 1d) is higher than that obtained under any static potentials, corresponding to an ∼1.6-fold enhancement in ORR when compared to the sum of charge of −0.9 and −0.3 V under static potential. The transient disk current response is shown in Figure S5. Note that the charge obtained in N_2-saturated solution was subtracted to remove the contribution from the non-Faradaic process (see SI section S4). The selectivity of H_2O_2 under this dynamic potential oscillation reaches $X_{H_2O_2}$ = 82.4 ± 0.3% (curve i in Figure 1e), representing a 1.23-fold increase compared with the expected selectivity based on the average of selectivity under static potentials. The calculation of expected selectivity via a weighted average of static conditions is described in SI Section S1. An example disk current response with potential oscillation is shown in Figure S6. Moreover, we observed that the H_2O_2 selectivity (measured as $X_{H_2O_2}$) under the oscillating potential between −0.6 V and −0.3 V at 100 Hz increased to 88.8 ± 0.2% compared to the 83.1 ± 0.2% at static −0.6 V (Figure S7). This suggests that the H_2O_2 selectivity can be increased without crossing −0.6 V, which shows the maximum H_2O_2 selectivity under a static potential. When we increase the duration of the upper potential (−0.3 V) during potential oscillation to 95 ms while keeping the duration for the lower potential (−0.9 V) at 5 ms, the H_2O_2 selectivity further reaches 90.7 ± 0.9%, which exceeds those attainable under any static potentials with otherwise the same conditions (curve ii in Figure 1e). An ∼3.1-fold increase in ORR activity (measured by the overall charge) is observed compared to the static potential (curve ii in Figure 1d). The enhancement in the ORR activity under dynamic potential oscillation is at least partially because of mass transfer. In the less negative potential half-cycle, the absence of significant ORR allows O_2 to transport from the bulk to supplement its depletion in the diffusion layer. The enhancement of the ORR current due to mass transport is demonstrated via finite element simulation, as shown by the concentration profile versus time in Figure S14, and the discussion in SI section S5. The superior selectivity for H_2O_2 under dynamic potential oscillation compared to any static conditions suggests that dynamic potential oscillation creates some unique interfacial environment that is not prevalent during static electrocatalysis, favoring H_2O_2.

We further studied the effect of the potential oscillation frequency on the selectivity and activity of the ORR. A potential oscillation at different frequencies (10 to 100 Hz) between −0.4 V and −0.9 V was applied to the Au rotating disk electrode for 15 s in O_2-saturated phosphate buffer (PB, pH 7.4). As illustrated in Figure 2a, the ORR activity exhibited a 1.5-fold increase under dynamic potential oscillation at 10 Hz compared to the activity under static potential. The ORR activity enhancement plateaus to ∼1.6-fold compared to the static condition when the frequency is >10 Hz.

The effect of the potential oscillation frequency on the selectivity of ORR toward H_2O_2 was verified using two methods: RRDE and fluorescence. The RRDE results in Figure 2b show that the selectivity toward H_2O_2 over H_2O is enhanced to 75% when the disk potential oscillates at 10 Hz

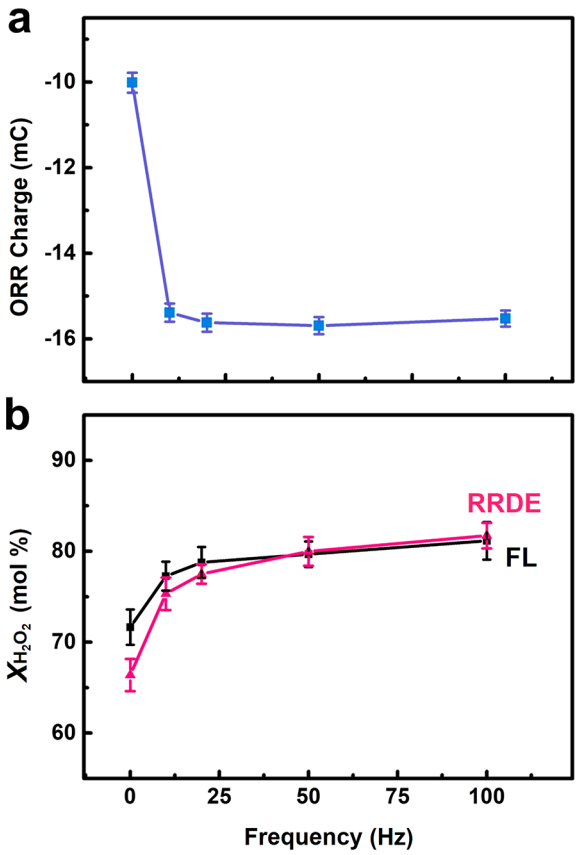

Figure 2. (a) ORR activity measured as the total charge from potential oscillation (−0.4 and −0.9 V) at different frequencies in RRDE in an O_2-saturated solution of 0.1 M PB (pH 7.4). (b) ORR selectivity measured as $X_{H_2O_2}$ via RRDE (red) and fluorescence (black). Rotation rate: 1200 rpm. The error bars indicate the standard deviation of the three independent measurements.

compared with static conditions. The selectivity further increases to >80% at 100 Hz. This increase in ORR selectivity to H_2O_2 under dynamic potential oscillation is further verified via a fluorescence assay of H_2O_2 based on horseradish peroxidase (HRP) and Amplex Red. A Au RDE was used as the working electrode instead of an RRDE to exclude the possibility of H_2O_2 decomposition on the Pt ring and the crosstalk between the Pt ring and Au disk in the RRDE (Figure S18). Additionally, the counter electrode was placed in a solution separated by a glass frit to avoid the reaction of H_2O_2 on the counter electrode. As shown in Figure 2b, the mole fraction of H_2O_2 detected using fluorescence quantitatively agrees with the RRDE experiments: the mole fraction of H_2O_2 increases from 72% under static conditions to ∼81% when the potential dynamically oscillates. The details about the fluorescence-based measurement of H_2O_2, including the calibration curve and the calculation of the mole fraction H_2O_2, are shown in Figure S16 and SI section S1.

We further performed bulk electrocatalysis to demonstrate that the effect of dynamic potential oscillation persists in longer times. Figure 3a shows that the ORR charge is ∼1.5× higher under the dynamic potential oscillation at 10 min and becomes ∼1.4× higher at 30 min. For a fair comparison, the time axis in Figure 3 represents the total time spent at −0.8 V because the charge at −0.3 V under dynamic conditions is negligible (see Figure 1c). The selectivity toward H_2O_2 at

https://doi.org/10.1021/jacs.3c13694
J. Am. Chem. Soc. XXXX, XXX, XXX−XXX

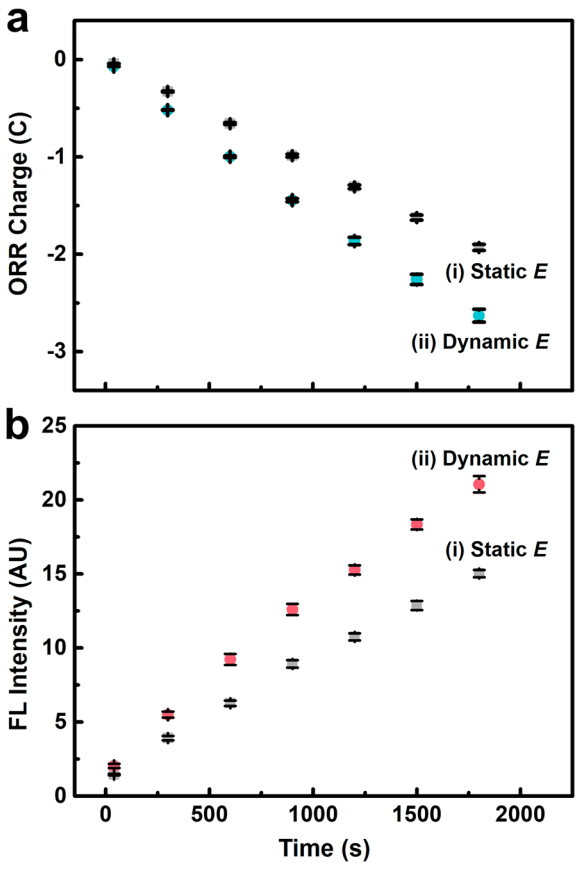

Figure 3. (a) Accumulated ORR charge on Au RDE and (b) fluorescence (FL) intensity for H_2O_2 detection under 9) static potential and (i) static (−0.8 V) and (ii) dynamic potentials (potential oscillation between −0.3 and −0.8 V at 10 Hz). Time represents to the duration at ORR operating potential (−0.8 V). The error bars show the standard deviation of three independent measurements.

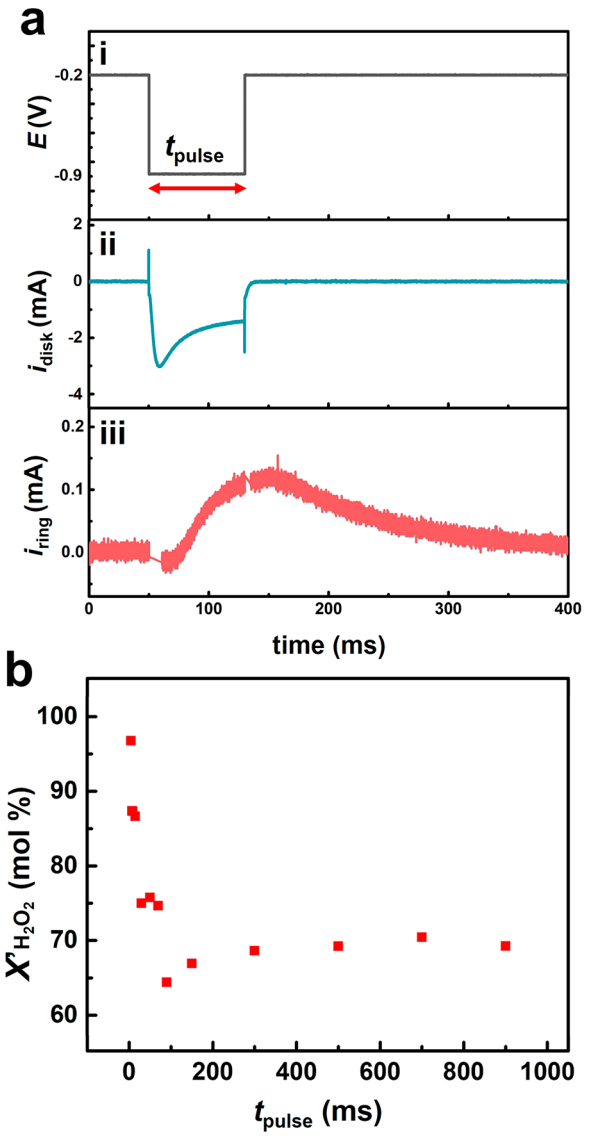

Figure 4. (a) (i) Waveform of a single pulse with a duration of t_{pulse} applied to the Au disk electrode. Corresponding current at (ii) the Au disk and (iii) Pt ring electrodes of RRDE. (b) Transient selectivity of the ORR measured by the mole fraction of H_2O_2 produced. Solution is O_2-bubbled 0.1 M PB (pH 7.4). Rotation rate: 1200 rpm. The noise from electronic cross-talk in the current is removed. See the raw data and discussion in SI Section S9.

different times in the bulk electrolysis is also monitored via fluorescence. The fluorescence intensity, proportional to H_2O_2 concentration, is consistently ∼1.4× higher under dynamic potential than under static potential throughout the experiment. These results further corroborate the enhancement of both ORR activity and H_2O_2 production under dynamic conditions vs static conditions at extended reaction time.

We hypothesize that the enhancement in H_2O_2 selectivity under dynamic potential occurs transiently, right after potential switching. To probe the time scale of the transient effect, we perform a transient RRDE experiment to measure the selectivity at different times after the potential step. Note that the finite transit time for H_2O_2 to transport from disk to the ring (e.g., ∼20 ms for 1200 rpm, see SI section 5c) makes it challenging to directly resolve the selectivity in real-time at shorter time scales (e.g., < 100 ms). Therefore, we generate single potential pulses on the disk with different durations (t_{pulse}) and collect H_2O_2 on the ring. As the waveform in Figure 4a(i) shows, the disk potential is initially at −0.2 V, where essentially no ORR occurs. At t = 0, the potential is stepped to −0.9 V for a duration of t_{pulse} to induce ORR. As shown in Figure 4a(ii), the current on the disk after subtracting the charging current shows that the ORR current reaches a peak in 8 ms after the potential step, which is consistent with the establishment of the electrode potential during charging.[20] The characteristic charging time can be represented by the RC time constant, which suggests that the potential is expected to reach 95% of the desired value after ∼4 ms (i.e., 3 times the RC time constant). See SI Section 8 for a detailed discussion about double layer charging. The current then decreases in a Cottrell-like manner and approaches the steady-state current. After 80 ms, the potential is switched back to −0.2 V, and the current quickly decays back to the baseline.

The ring is held at the potential for H_2O_2 collection even after the pulse on the disk is complete so that the total H_2O_2 generated from different pules can be calculated. As shown in Figure 4a(iii), the ring current lags the disk current by ∼20 ms, consistent with the expected transit time between the disk and the ring (Figure S11). The current continues to increase and reaches a maximum at ∼95 ms after the start of the potential pulse. The ring current then decays back to the baseline in

https://doi.org/10.1021/jacs.3c13694
J. Am. Chem. Soc. XXXX, XXX, XXX−XXX

~200 ms. This profile matches well with that expected from finite element simulation (Figure S12). The total H_2O_2 produced for different pulse duration can be measured by integrating the overall ring current, and the resulting charge can be used to obtain the average selectivity to H_2O_2. Further differentiation of the average selectivity versus time yields the transient selectivity at different times. The data processing details to obtain the transient selectivity are shown in SI Section S6. As shown in Figure 4b, ORR selectivity toward H_2O_2 is higher in the shorter time scale. For example, up to 97% of the product is H_2O_2 within the first 5 ms. The selectivity decreases at a longer time, reaching a plateau of 69% at >500 ms, which is similar to the selectivity under the static −0.9 V. This result confirms that enhancement of H_2O_2 selectivity mostly occurs in this transient region (within the first 100 ms), which explains why the overall H_2O_2 production increases with frequency during potential oscillation. On the other hand, the finite RC time constant on the electrode limits us from properly interpreting the electrode potential and current response when the time scale is shorter than the three times of RC time constant. Therefore, we did not explore frequencies higher than 100 Hz.

As discussed in the introduction, the key step in controlling the selectivity in the ORR is the bond breakage of the adsorbed intermediate *OOH. Specifically, if the *−OOH bond is weakened, the reductive desorption will lead to H_2O_2. On the other hand, if the *O−OH bond is cleaved instead, the final product will be H_2O. Other spectator adsorbed species, especially anions, are known to change both the activity and selectivity of ORR on Au.[21] Oxo-anions like phosphate can lower ORR activity while shifting the products toward H_2O_2.[18,22] As shown in Figure 5a, when ClO_4^- is the primary anion, which shows very weak to no adsorption on Au, the dynamic condition results in lower H_2O_2 selectivity. In the presence of SO_4^{2-}, which is strongly adsorbed on Au, the dynamic condition also results in lower H_2O_2 selectivity. Therefore, the adsorption strength alone cannot explain the increased selectivity under the dynamic conditions. The adsorbed phosphate (HPO_4^{2-} and $H_2PO_4^-$) likely helps regulate the proton near the interface, allowing the protonation of the terminal oxygen directly attached to the surface and facilitating the desorption of peroxide. Given that we have demonstrated that the enhancement to H_2O_2 occurs in the shorter time scale (<100 ms), the proposed overall mechanism for the increase of H_2O_2 production under dynamic conditions with phosphate buffer is consistent with the proposed mechanism in Scheme 1: at the more positive potential where essentially no ORR occurs, the adsorption of phosphate is facilitated. When the potential is transiently switched to more negative potentials, phosphate is transiently present at the surface, facilitating the protonation of *OOH and desorption of peroxide and increasing the selectivity to H_2O_2.

We also compared the selectivity toward H_2O_2 in RRDE at different concentrations of phosphate buffer (pH 7.1) and perchlorate anion while maintaining the same ionic strength of the solution (0.224 M). Figure 5b shows that the H_2O_2 selectivity decreases under dynamic conditions when the phosphate buffer is below 5 mM. While the selectivity to H_2O_2 under both dynamic potentials and static potentials increases as the phosphate buffer concentration increases, an H_2O_2 selectivity is higher under dynamic potential conditions when phosphate buffer exceeds 10 mM. This further suggests the role of phosphate in the tuning of ORR selectivity under dynamic potential oscillation conditions.

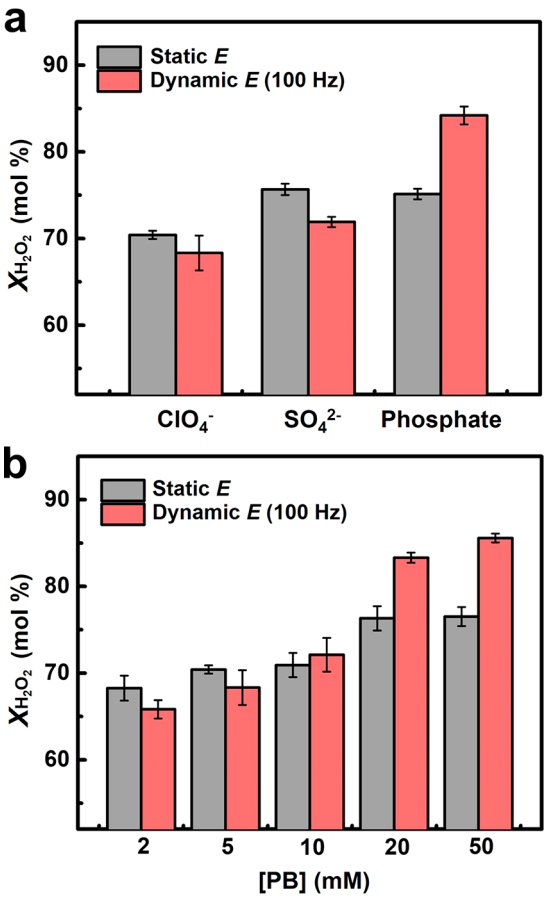

Figure 5. (a) Effect of anion on the H_2O_2 selectivity under static and dynamic conditions. Solution: O_2-saturaed solution containing NaY (Y= perchlorate, sulfate, and phosphate) and 5 mM phosphate buffer. (b) Effect of phosphate buffer concentration on H_2O_2 selectivity. The ionic strength of all solutions is kept constant at 0.224 M via the addition of $NaClO_4$. Solution pH is 7.1. Static *E*: constant potential at −0.8 V. Dynamic *E*: potential oscillation between −0.3 V and −0.8 V at 100 Hz. The error bars exhibit the standard deviations of three independent measurements.

Lastly, we rule out the contribution of pH effect on ORR. It is known that ORR on Au(100) shifts from the 4-electron pathway in alkaline media to the 2-electron pathway in acidic media.[21] It is expected that the pH change will be less under dynamic conditions because mass transfer at the less negative potential part during potential oscillation helps reverse the pH increase from the ORR. Therefore, when the buffer is weak, the dynamic condition should create a lower average interfacial pH compared with static potential condition, which should favor H_2O_2 generation. When the buffer strength increases, this dynamic pH effect should decrease. However, this trend is the opposite of the increase in H_2O_2 selectivity under dynamic potential oscillation when the buffer strength increases, as shown in Figure 5b.

CONCLUSION

In conclusion, we have shown that the selectivity and activity of the ORR can be tuned by dynamically oscillating the electrode potential at the same electrocatalytic surface. Importantly, by working in well-defined mass transport

https://doi.org/10.1021/jacs.3c13694
J. Am. Chem. Soc. XXXX, XXX, XXX−XXX

Scheme 1. Dynamic Interface Created by Potential Oscillation to Affect Electrocatalytic Oxygen Reduction Reaction

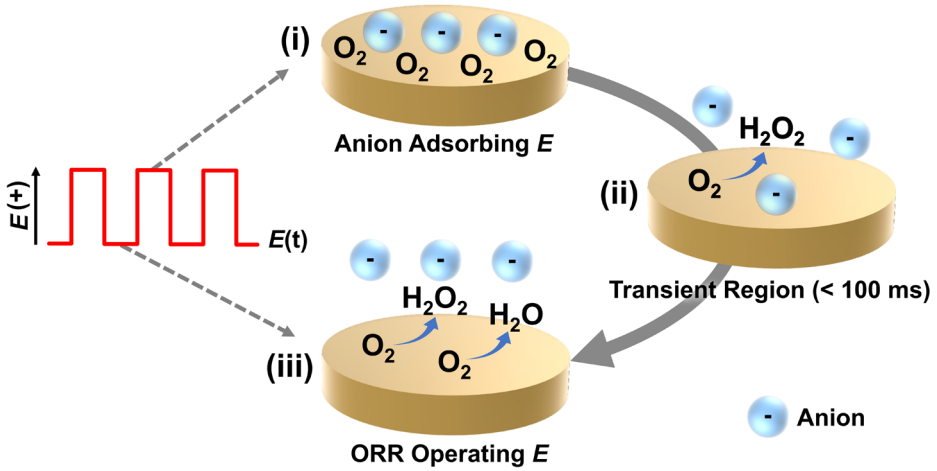

conditions, we demonstrate that the selectivity toward H_2O_2 under dynamic potential oscillation can exceed that of any static potential under similar conditions. The results suggest that a unique interfacial environment to favor H_2O_2 generation can be created under dynamic electrocatalysis transiently, which is not accessible under static potential conditions. Specifically, the adsorption and desorption of phosphate under potential oscillation can increase the selectivity of ORR toward H_2O_2 by 1.35 times compared with the static potential conditions. The increased selectivity is experimentally shown to occur transiently in the time scale of milliseconds or shorter. The transient selectivity to H_2O_2 on Au can reach ~97% within the first 5 ms. The observed results are consistent with the mechanism of the transient adsorption of phosphate facilitated by dynamic potential oscillation to promote the protonation and desorption of *−OOH, leading to enhanced H_2O_2 generation. The use of Au as a model electrode can facilitate further spectroelectrochemistry of the interface. Overall, our work demonstrates that using the dynamical electrochemical interface to create unique microenvironments can add a new dimension to electrocatalysis design, offering new activity and selectivity at the electrocatalysts.

■ ASSOCIATED CONTENT

Supporting Information

The Supporting Information is available free of charge at https://pubs.acs.org/doi/10.1021/jacs.3c13694.

Experimental section, RRDE behavior, finite element simulation, selectivity calculation, H_2O_2 quantification, RC time constant, and data processing (PDF)

■ AUTHOR INFORMATION

Corresponding Author

Hang Ren − *Department of Chemistry, The University of Texas at Austin, Austin, Texas 78712, United States; Center for Electrochemistry and Texas Materials Institute, The University of Texas at Austin, Austin, Texas 78712, United States;* orcid.org/0000-0002-9480-8881; Phone: hren@utexas.edu

Author

Hyein Lee − *Department of Chemistry, The University of Texas at Austin, Austin, Texas 78712, United States*

Complete contact information is available at: https://pubs.acs.org/10.1021/jacs.3c13694

Notes

The authors declare no competing financial interest.

■ ACKNOWLEDGMENTS

We acknowledge Dr. Richard M. Crooks and Dr. Yuanyue Liu for their insightful discussion. H.R. acknowledges the support from the Chemical Measurement & Imaging Program (CMI) at the National Science Foundation under Grant No. CHE-2240113, and the start-up fund from UT Austin.

■ REFERENCES

(1) Chu, S.; Majumdar, A. Opportunities and challenges for a sustainable energy future. *Nature* **2012**, *488* (7411), 294−303.

(2) Campos-Martin, J. M.; Blanco-Brieva, G.; Fierro, J. L. G. Hydrogen Peroxide Synthesis: An Outlook beyond the Anthraquinone Process. *Angew. Chem., Int. Ed.* **2006**, *45* (42), 6962−6984.

(3) Verdaguer-Casadevall, A.; Deiana, D.; Karamad, M.; Siahrostami, S.; Malacrida, P.; Hansen, T. W.; Rossmeisl, J.; Chorkendorff, I.; Stephens, I. E. L. Trends in the Electrochemical Synthesis of H_2O_2: Enhancing Activity and Selectivity by Electrocatalytic Site Engineering. *Nano Lett.* **2014**, *14* (3), 1603−1608.

(4) Akbashev, A. R. Electrocatalysis Goes Nuts. *ACS Catal.* **2022**, *12* (8), 4296−4301.

(5) Seh, Z. W.; Kibsgaard, J.; Dickens, C. F.; Chorkendorff, I.; Nørskov, J. K.; Jaramillo, T. F. Combining theory and experiment in electrocatalysis: Insights into materials design. *Science* **2017**, *355* (6321), eaad4998.

(6) Grabow, L. C.; Hvolbæk, B.; Nørskov, J. K. Understanding Trends in Catalytic Activity: The Effect of Adsorbate-Adsorbate Interactions for CO Oxidation Over Transition Metals. *Top. Catal.* **2010**, *53* (5), 298−310.

(7) Lausche, A. C.; Medford, A. J.; Khan, T. S.; Xu, Y.; Bligaard, T.; Abild-Pedersen, F.; Nørskov, J. K.; Studt, F. On the effect of coverage-dependent adsorbate-adsorbate interactions for CO methanation on transition metal surfaces. *J. Catal.* **2013**, *307*, 275−282.

(8) Ardagh, M. A.; Abdelrahman, O. A.; Dauenhauer, P. J. Principles of Dynamic Heterogeneous Catalysis: Surface Resonance and Turnover Frequency Response. *ACS Catal.* **2019**, *9* (8), 6929−6937.

(9) Ardagh, M. A.; Shetty, M.; Kuznetsov, A.; Zhang, Q.; Christopher, P.; Vlachos, D. G.; Abdelrahman, O. A.; Dauenhauer, P. J. Catalytic resonance theory: parallel reaction pathway control. *Chem. Sci.* **2020**, *11* (13), 3501−3510.

(10) Shetty, M.; Walton, A.; Gathmann, S. R.; Ardagh, M. A.; Gopeesingh, J.; Resasco, J.; Birol, T.; Zhang, Q.; Tsapatsis, M.;

Vlachos, D. G.; et al. The Catalytic Mechanics of Dynamic Surfaces: Stimulating Methods for Promoting Catalytic Resonance. *ACS Catal.* **2020**, *10* (21), 12666−12695.
(11) Gopeesingh, J.; Ardagh, M. A.; Shetty, M.; Burke, S. T.; Dauenhauer, P. J.; Abdelrahman, O. A. Resonance-Promoted Formic Acid Oxidation via Dynamic Electrocatalytic Modulation. *ACS Catal.* **2020**, *10* (17), 9932−9942.
(12) Kimura, K. W.; Casebolt, R.; Cimada DaSilva, J.; Kauffman, E.; Kim, J.; Dunbar, T. A.; Pollock, C. J.; Suntivich, J.; Hanrath, T. Selective Electrochemical CO_2 Reduction during Pulsed Potential Stems from Dynamic Interface. *ACS Catal.* **2020**, *10* (15), 8632−8639.
(13) Timoshenko, J.; Bergmann, A.; Rettenmaier, C.; Herzog, A.; Arán-Ais, R. M.; Jeon, H. S.; Haase, F. T.; Hejral, U.; Grosse, P.; Kühl, S.; et al. Steering the structure and selectivity of CO_2 electroreduction catalysts by potential pulses. *Nat. Catal.* **2022**, *5* (4), 259−267.
(14) Zhang, X.-D.; Liu, T.; Liu, C.; Zheng, D.-S.; Huang, J.-M.; Liu, Q.-W.; Yuan, W.-W.; Yin, Y.; Huang, L.-R.; Xu, M.; et al. Asymmetric Low-Frequency Pulsed Strategy Enables Ultralong CO_2 Reduction Stability and Controllable Product Selectivity. *J. Am. Chem. Soc.* **2023**, *145* (4), 2195−2206.
(15) Ding, Y.; Zhou, W.; Xie, L.; Chen, S.; Gao, J.; Sun, F.; Zhao, G.; Qin, Y. Pulsed electrocatalysis enables an efficient 2-electron oxygen reduction reaction for H_2O_2 production. *J. Mater. Chem. A* **2021**, *9* (29), 15948−15954.
(16) Ding, Y.; Zhou, W.; Li, J.; Wang, J.; Xie, L.; Meng, X.; Gao, J.; Sun, F.; Zhao, G.; Qin, Y. Revealing the In Situ Dynamic Regulation of the Interfacial Microenvironment Induced by Pulsed Electrocatalysis in the Oxygen Reduction Reaction. *ACS Energy Lett.* **2023**, *8* (7), 3122−3130.
(17) Shao, M.; Chang, Q.; Dodelet, J.-P.; Chenitz, R. Recent Advances in Electrocatalysts for Oxygen Reduction Reaction. *Chem. Rev.* **2016**, *116* (6), 3594−3657.
(18) Prieto, A.; Hernández, J.; Herrero, E.; Feliu, J. M. The role of anions in oxygen reduction in neutral and basic media on gold single-crystal electrodes. *J. Solid State Electrochem.* **2003**, *7* (9), 599−606.
(19) Sánchez-Sánchez, C. M.; Bard, A. J. Hydrogen Peroxide Production in the Oxygen Reduction Reaction at Different Electrocatalysts as Quantified by Scanning Electrochemical Microscopy. *Anal. Chem.* **2009**, *81* (19), 8094−8100.
(20) Bard, A. J.; Faulkner, L. R.; White, H. S. *Electrochemical Methods: Fundamentals and Applications*; Wiley: 2022.
(21) Blizanac, B. B.; Lucas, C. A.; Gallagher, M. E.; Arenz, M.; Ross, P. N.; Marković, N. M. Anion Adsorption, CO Oxidation, and Oxygen Reduction Reaction on a Au(100) Surface: The pH Effect. *J. Phys. Chem. B* **2004**, *108* (2), 625−634.
(22) Wang, J. X.; Markovic, N. M.; Adzic, R. R. Kinetic Analysis of Oxygen Reduction on Pt(111) in Acid Solutions: Intrinsic Kinetic Parameters and Anion Adsorption Effects. *J. Phys. Chem. B* **2004**, *108* (13), 4127−4133.

https://doi.org/10.1021/jacs.3c13694
J. Am. Chem. Soc. XXXX, XXX, XXX−XXX